AD NUMBER
AD005941
CLASSIFICATION CHANGES
TO: unclassified
FROM: confidential
LIMITATION CHANGES
TO: Approved for public release, distribution unlimited
FROM: Distribution authorized to U.S. Gov't. agencies and their contractors; Administrative/Operational Use; 06 APR 1953. Other requests shall be referred to National Aeronautics and Space Administration, Washington, DC.
AUTHORITY
NASA TR Server website; NASA TR Server website

AD- 5941

CONFIDENTIAL

RESEARCH MEMORANDUM

TRANSONIC WIND-TUNNEL INVESTIGATION OF THE AERODYNAMIC CHARACTERISTICS OF A 60° TRIANGULAR WING IN COMBINATION WITH A SYSTEMATIC SERIES OF THREE BODIES

By Thomas C. Kelly

Langley Aeronautical Laboratory
Langley Field, Va.

NATIONAL ADVISORY COMMITTEE
FOR AERONAUTICS

WASHINGTON
April 6, 1953

NATIONAL ADVISORY COMMITTEE FOR AERONAUTICS

RESEARCH MEMORANDUM

TRANSONIC WIND-TUNNEL INVESTIGATION OF THE AERODYNAMIC CHARACTERISTICS OF A 60° TRIANGULAR WING IN COMBINATION WITH A SYSTEMATIC SERIES OF THREE BODIES

By Thomas C. Kelly

SUMMARY

Aerodynamic characteristics and the effect of body shape on wing-fuselage interference are presented for a 60° triangular wing at Mach numbers from 0.60 to 1.125 and angles of attack from 0° to 7°. Basic aerodynamic characteristics are also presented for the wing with interference of one configuration through the same Mach number range and at angles of attack to 24°. The results indicate that the addition of a cylindrical afterbody to a normal curved fuselage markedly reduced the transonic zero-lift drag rise and increased the maximum lift-drag ratio in the supersonic range for the wing with interference. Additions of the cylindrical afterbody and the cylindrical afterbody in combination with an extended forebody generally resulted in an increase in the drag due to lift for the wing with interference. Lift and pitching moment were relatively unaffected by modifications to the normal curved fuselage.

INTRODUCTION

Previous papers have presented the aerodynamic characteristics of triangular wings at subsonic and supersonic speeds, but only a limited amount of data is available for these wings in the transonic range at lifting conditions. As part of a general wing-fuselage-interference program being conducted in the Langley 8-foot transonic tunnel, the basic aerodynamic characteristics at angles of attack to 24° and the effects of several basic changes in body shape on wing-fuselage interference at angles of attack from 0° to 7° have been obtained at Mach numbers from 0.60 to 1.125 for a thin triangular wing which had 60° sweepback of the leading edge, an aspect ratio of 2.31, and an NACA 65A002 airfoil section parallel to the plane of symmetry. Results

of investigations of representative swept and unswept wings in combination with these same bodies are presented in references 1 and 2.

SYMBOLS

M	average stream Mach number
q	free-stream dynamic pressure, lb/sq ft
$\bar{c}$	wing mean aerodynamic chord, in.
S	wing area, sq ft
C_L	lift coefficient, $\frac{\text{Lift}}{qS}$
C_D	drag coefficient, $\frac{\text{Drag}}{qS}$
C_m	pitching-moment coefficient, $\frac{\text{Pitching moment about } 0.25\bar{c}}{qS\bar{c}}$
$\left(\frac{dC_L}{d\alpha}\right)_{av}$	lift-curve slope per degree, averaged over a lift-coefficient range of 0 to 0.4
$\left(\frac{\partial C_m}{\partial C_L}\right)_{av}$	static-longitudinal-stability parameter, averaged over a lift-coefficient range of 0 to 0.4
$(L/D)_{max}$	maximum lift-drag ratio
P_b	base pressure coefficient, $\frac{p_b - p}{q}$
ΔP_b	incremental base pressure coefficient due to addition of wing to fuselage
p	free-stream static pressure, lb/sq ft
p_b	static pressure at model base, lb/sq ft
α	angle of attack of fuselage axis, deg

APPARATUS AND METHODS

Tunnel

The Langley 8-foot transonic tunnel is a single-return, slotted-throat wind tunnel capable of continuous operation through the speed range up to a Mach number of about 1.13. A complete description of the Langley 8-foot transonic tunnel may be found in reference 3.

Models

Wing.- Three configurations, differing only in fuselage shape, were used for the present investigation. The wing used in all three combinations (see fig. 1) had 60° sweepback of the leading edge, an aspect ratio of 2.31, a taper ratio of 0, and an NACA 65A002 airfoil section parallel to the plane of symmetry. The wing area, including the part of the wing enclosed in the fuselage, was 1 square foot. Wing construction was of stainless steel.

Fuselages.- The basic combination, designated as configuration A, had a fuselage designed by cutting off the rear portion of a body of revolution with a basic fineness ratio of 12 to form a body with a fineness ratio of 9.8. The fuselage of configuration B was obtained by the addition of a plastic cylindrical section to configuration A which extended from the fuselage maximum diameter to the model base. The fuselage of configuration C was formed by the addition of a second cylindrical plastic section to configuration B which extended the original forebody upstream a distance equal to twice the fuselage maximum diameter. Ordinates for the three fuselages are presented in reference 1. It should be noted that fuselage configurations A, B, and C of the present investigation correspond to bodies A, C, and D, respectively, of reference 1. Body configuration B of reference 1 was not included in the present investigation due to a lack of available tunnel testing time.

Sting configurations.- Models were mounted on an internal strain-gage balance. The rear portion of the balance comprised a sting for supporting the model in the tunnel. For the original afterbody (configuration A) the sting was tapered from the base of the model rearward (see fig. 1). The sting rearward from the base of the cylindrical afterbody configuration had a cylindrical cross section with a constant diameter slightly less than that of the body (fig. 1). A photograph of configuration B mounted in the slotted test section of the Langley 8-foot transonic tunnel is presented as figure 2.

Measurements and Accuracy

Lift, drag, and pitching moment were measured by means of the internal strain-gage balance. Coefficients are based on the total wing area of 1 square foot. Pitching-moment coefficients, based on a mean aerodynamic chord of 10.529 inches, are referred to the quarter point of the mean aerodynamic chord.

Measured coefficients for the various configurations are estimated to be accurate within the following limits:

Configurations A and B:

	Low speeds	High speeds
C_L	±0.008	±0.004
C_D	±0.001	±0.0005
C_m	±0.003	±0.002

Configuration C:

	Low speeds	High speeds
C_L	±0.016	±0.008
C_D	±0.005	±0.002
C_m	±0.002	±0.002

The difference in estimated accuracy for configuration C was caused by the use of a stronger balance with this configuration to allow testing at the higher angles. It should be noted that the limits presented represent maximum estimated errors for the measured coefficients and when based upon scatter and repeatability of data would be considerably lower.

The angle of attack of the model was measured with an optical system sighted on a reference line on the fuselage and is estimated to be accurate within $\pm 0.1^\circ$. Angles of attack at which data were recorded are shown in figure 3.

Local deviations from the average free-stream Mach number did not exceed 0.003 at subsonic Mach numbers and did not become greater than 0.010 with increases in Mach number to 1.125.

Static pressure at the rear end of the models was obtained from pressure orifices located in the top and bottom of the sting support in the plane of the model base.

Average Reynolds number for the present investigation, based on the mean aerodynamic chord, varied from approximately 2.9×10^6 to 3.5×10^6.

The effects of boundary-reflected disturbances in the slotted test section of the Langley 8-foot transonic tunnel on the results presented were small (refs. 3 and 4) and the drag data presented at constant lift coefficient have been faired in an attempt to eliminate these effects. The faired data presented never differed from the actual data by more than 0.001 in drag coefficient.

RESULTS AND DISCUSSION

The various body shapes used in the present investigation were developed to reduce the effects of interference between the wing and body. The forebody was extended in an attempt to reduce the induced velocities produced by the body in the region of the forward portion of the wing. The cylindrical afterbody was added in an attempt to reduce the induced velocities produced by the original afterbody in the region of the rear part of the wing. These changes made in body shape were of a basic research nature and were not meant to suggest practical configurations.

All data presented, unless otherwise noted, are for the wing with interference and were obtained by subtracting the body-alone data of reference 1 from the corresponding combination data of the present investigation. The results have been adjusted to a condition at which the static pressure at the model base and the free-stream static pressure are equal. Base pressure coefficients for the wing-fuselage combinations and incremental base pressure coefficients due to the addition of the wing to the fuselage of the combinations are presented in figure 3. Basic data are presented as angle of attack, drag coefficient, and pitching-moment coefficient as a function of lift coefficient in figure 4. From these basic data the analysis figures have been prepared.

Lift Characteristics

The variation with lift coefficient of angle of attack for the three configurations is presented in figure 4(a). There are indications of a break which occurs in the lift curve for configuration C at Mach numbers from 0.80 to 0.90 and an angle of attack of approximately 13°. Similar breaks may be noted in the data of references 5 and 6. Variation with Mach number of average lift-curve slopes for the three configurations is presented in figure 5. The addition of a cylindrical afterbody (configuration B) to the basic fuselage (configuration A) resulted in a decrease in the values of $\left(\frac{dC_L}{d\alpha}\right)_{av}$ throughout the Mach number range with a decrease of 10 percent noted at Mach numbers near 1.0. Addition of an extended forebody (configuration C) produced no further

change. The addition of the cylindrical afterbody undoubtedly caused a reduction in the induced velocities over the aft portion of the wing. The resulting increased adverse pressure gradient over the forward part of the wing may have caused an increase in boundary-layer thickness over the upper surface of the wing at lifting conditions.

Drag Characteristics

Drag at constant lift coefficients.- The variation of drag coefficient with lift coefficient for several Mach numbers is presented in figure 4(b). Variation of drag coefficient with Mach number at constant lift is presented in figure 6. At zero lift coefficient, the wing with interference of configuration A experienced a drag rise of 0.004 starting at a Mach number of 0.95. Addition of a cylindrical afterbody to the basic fuselage resulted in a marked reduction of the drag rise due to the reduction of adverse wing-fuselage interference. A similar reduction in the zero-lift drag rise resulted from the addition of a cylindrical afterbody to the swept wing-body combination of reference 7. This reduction of the drag rise may be explained by application of the transonic-drag-rise concept (ref. 7) which indicates that the drag rise at transonic Mach numbers is a function of the axial cross-sectional area development of a particular configuration. Area developments for the three configurations are shown in figure 7 and it is apparent that the area development (in this case, reductions in cross-sectional area) over the rear portions of configuration B is much less severe than that over the same portion of configuration A. Addition of an extended forebody produced no further measurable change in the drag at zero lift throughout the Mach number range investigated.

At a lift coefficient of 0.2, the addition of a cylindrical afterbody (configuration B) to the basic fuselage resulted in an increase in drag at Mach numbers to about 0.975 for the wing with interference and a slight decrease in drag at the higher Mach numbers. These variations in drag were probably due to the same factors which affected the variations in lift-curve slope noted previously. Addition of an extended forebody (configuration C) increased the drag still further throughout the speed range. An increase in forebody length leads to an increase in the local upflow, increased adverse pressure gradients, and increased boundary-layer thickness near the leading edge of the wing root sections. Each of these effects would tend to influence leading-edge separation and over-all drag.

At a lift coefficient of 0.35, increases in stream Mach number were accompanied by a decrease in leading-edge separation with a resultant decrease in drag, as might be expected from previous results for swept wings (see ref. 8).

Maximum lift-drag ratios.- The effect of fuselage shape on maximum lift-drag ratio and lift coefficient for $(L/D)_{max}$ is shown in figure 8. The addition of a cylindrical afterbody (configuration B) to the original curved fuselage resulted in an improvement of $(L/D)_{max}$ at supersonic Mach numbers. Because the maximum lift-drag ratios were obtained at lift coefficients near 0.1, the values of $(L/D)_{max}$ are controlled to a considerable extent by the effects of body shape on drag near zero lift. It has been shown in figure 6 that the addition of a cylindrical afterbody reduced the drag at supersonic Mach numbers and lift coefficients of 0 and 0.2. The addition of an extended forebody (configuration C) resulted in a marked decrease in $(L/D)_{max}$ throughout the range.

Figure 9 has been obtained by the addition of an increment of drag coefficient of 0.01 to the wing with interference drag representing the additional drag due to a fuselage, tail, canopy, and so forth. For this case, the maximum lift-drag ratios were obtained at the higher lift coefficients $(C_L \approx 0.2)$ and the general levels of $(L/D)_{max}$ are reduced throughout the range to values closer to those that might be expected for a real airplane configuration. At subsonic Mach numbers, the values of $(L/D)_{max}$ are considerably lower than the values obtained for swept and unswept wings but, at transonic Mach numbers, are about the same as those obtained for such wings (refs. 1 and 2).

Pitching-moment characteristics.- The variation of pitching-moment coefficient with lift coefficient, shown in figure 4(c), is fairly linear except at the higher lift coefficients for configuration C at Mach numbers from 0.80 to 0.90 where a rearward shift in center-of-pressure location may be noted. At Mach numbers of 0.60 and 0.90, there are slight indications of a break which is associated with the lift-curve break shown in figure 4(a). Variation with Mach number of the average static-longitudinal-stability parameter $\partial C_m/\partial C_L$ (fig. 10) was only slightly affected by modifications made to the basic fuselage configuration.

CONCLUSIONS

The investigation of a 60° triangular wing in combination with a systematic series of three body shapes has led to the following conclusions relative to wing-body interference:

1. The drag rise at zero lift of the wing with interference when tested in combination with the original curved fuselage was markedly reduced by use of a cylindrical afterbody in combination with the wing.

2. Additions of the cylindrical afterbody and the cylindrical afterbody in combination with an extended forebody generally resulted in an increase in the drag due to lift for the wing with interference.

3. The use of a cylindrical afterbody in combination with the wing resulted in an increase in the maximum lift-drag ratio at supersonic Mach numbers for the wing with wing-fuselage interference.

4. Interference effects of the various body modifications on lift and pitching moment of the wing were small at all angles tested.

Langley Aeronautical Laboratory,
National Advisory Committee for Aeronautics,
Langley Field, Va.

REFERENCES

1. Loving, Donald L., and Wornom, Dewey E.: Transonic Wind-Tunnel Investigation of the Interference Between a 45° Sweptback Wing and a Systematic Series of Four Bodies. NACA RM L52J01, 1952.

2. Estabrooks, Bruce B.: Transonic Wind-Tunnel Investigation of an Unswept Wing in Combination With a Systematic Series of Four Bodies. NACA RM L52K12a, 1953.

3. Ritchie, Virgil S., and Pearson, Albin O.: Calibration of the Slotted Test Section of the Langley 8-Foot Transonic Tunnel and Preliminary Experimental Investigation of Boundary-Reflected Disturbances. NACA RM L51K14, 1952.

4. Osborne, Robert S., and Mugler, John P., Jr.: Aerodynamic Characteristics of a 45° Sweptback Wing-Fuselage Combination and the Fuselage Alone Obtained in the Langley 8-Foot Transonic Tunnel. NACA RM L52E14, 1952.

5. Smith, Donald W., and Heitmeyer, John C.: Lift, Drag, and Pitching Moment of Low-Aspect-Ratio Wings at Subsonic and Supersonic Speeds - Plane Triangular Wing of Aspect Ratio 2 With NACA 0005-63 Section. NACA RM A50K21, 1951.

6. Hall, Albert W., and McKay, James M.: The Effects on the Aerodynamic Characteristics of Varying the Wing Thickness Ratio of a Triangular Wing-Body Configuration at Transonic Speeds From Tests by the NACA Wing-Flow Method. NACA RM L52B18, 1952.

7. Whitcomb, Richard T.: A Study of the Zero-Lift Drag-Rise Characteristics of Wing-Body Combinations Near the Speed of Sound. NACA RM L52H08, 1952.

8. Whitcomb, Richard T., and Kelly, Thomas C.: A Study of the Flow Over a 45° Sweptback Wing-Fuselage Combination at Transonic Mach Numbers. NACA RM L52D01, 1952.

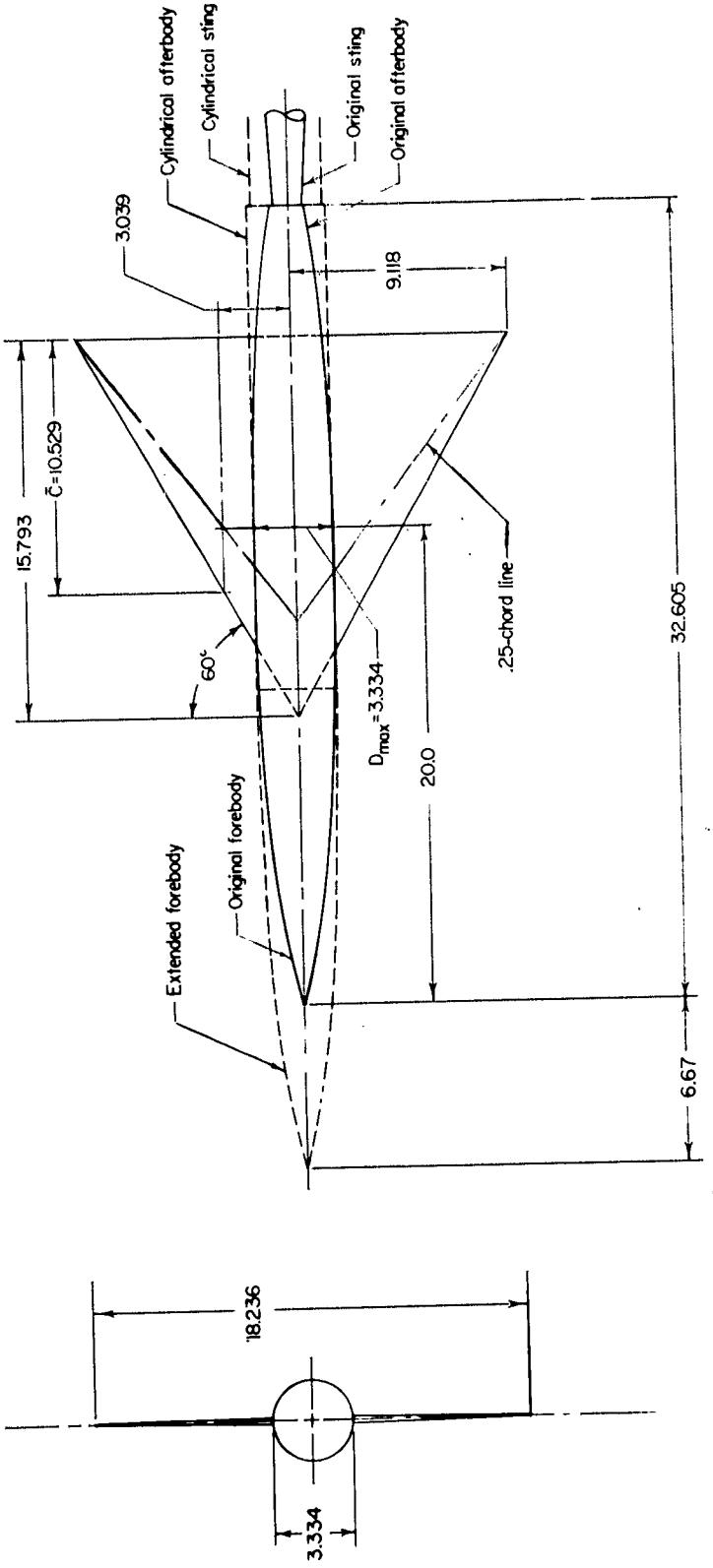

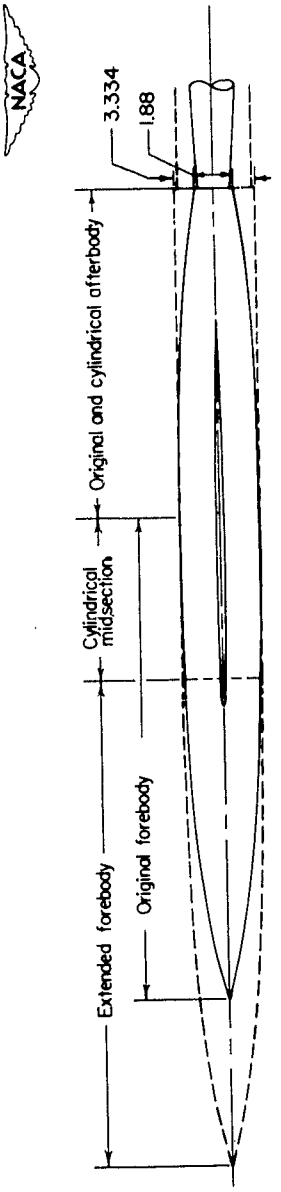

Wing Details	
Airfoil section (parallel to plane of symetry)	NACA 65A002
Area, sq ft	1
Aspect ratio	2.31
Taper ratio	0
Incidence, deg	0
Dihedral, deg	0

Figure 1.- Details of the various wing-fuselage configurations. All dimensions are in inches.

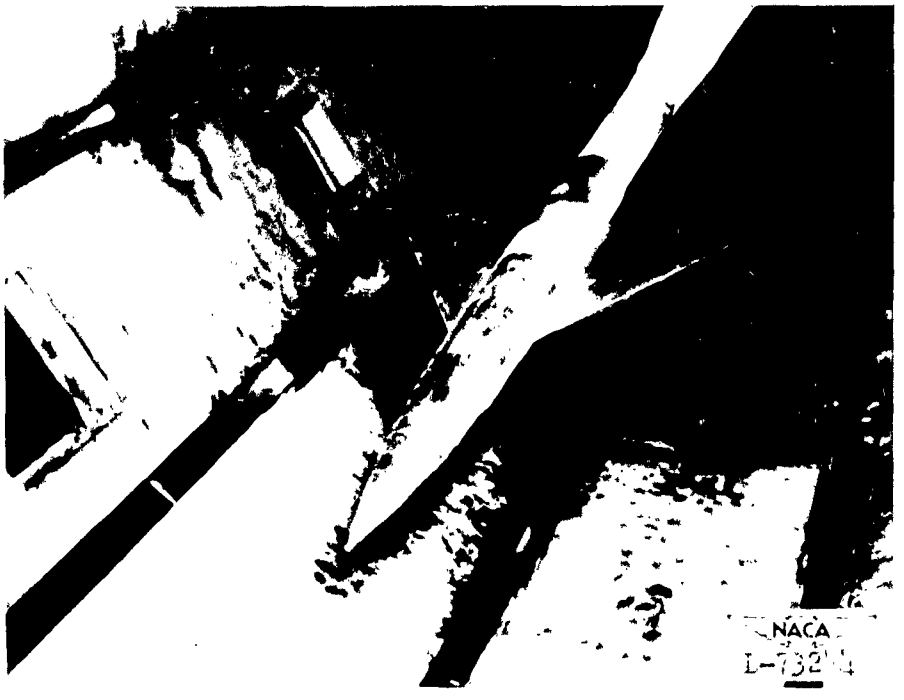

Figure 2.- Configuration B mounted in the slotted test section of Langley 8-foot transonic tunnel.

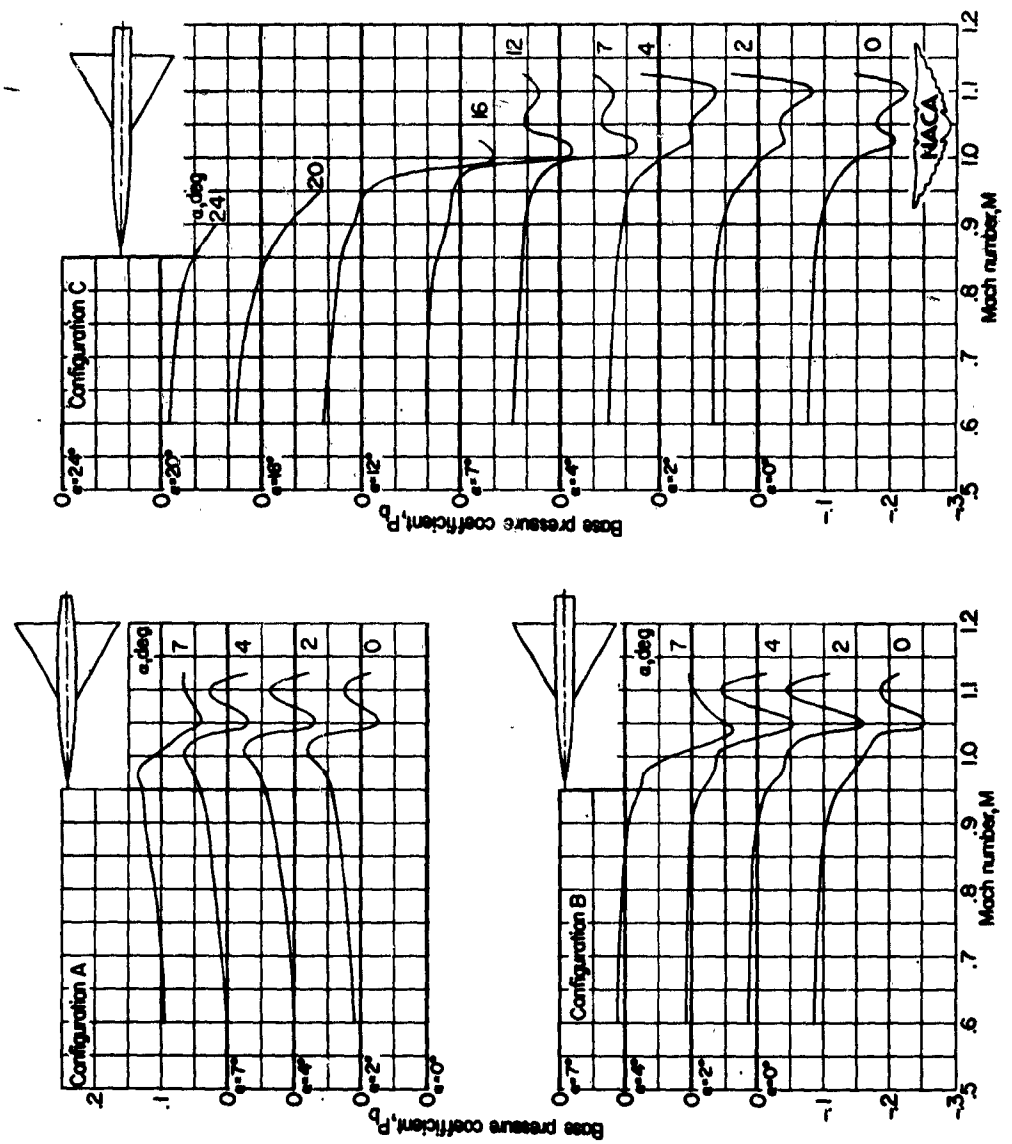

(a) Wing-fuselage combinations.

Figure 3.- Variation with Mach number of base pressure coefficient for the various configurations tested.

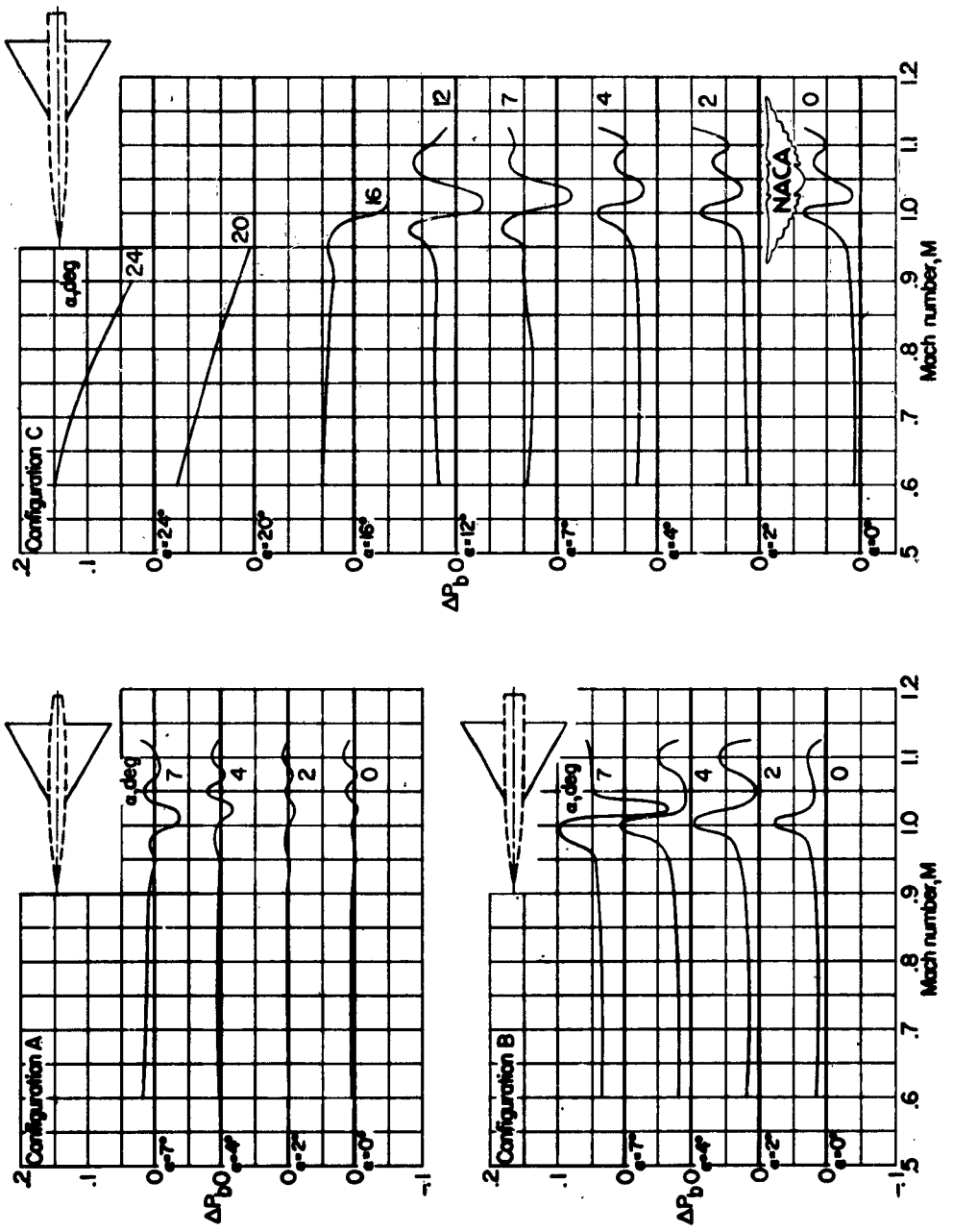

(b) Wing influence on base pressure coefficient of the various configurations.

Figure 3.- Concluded.

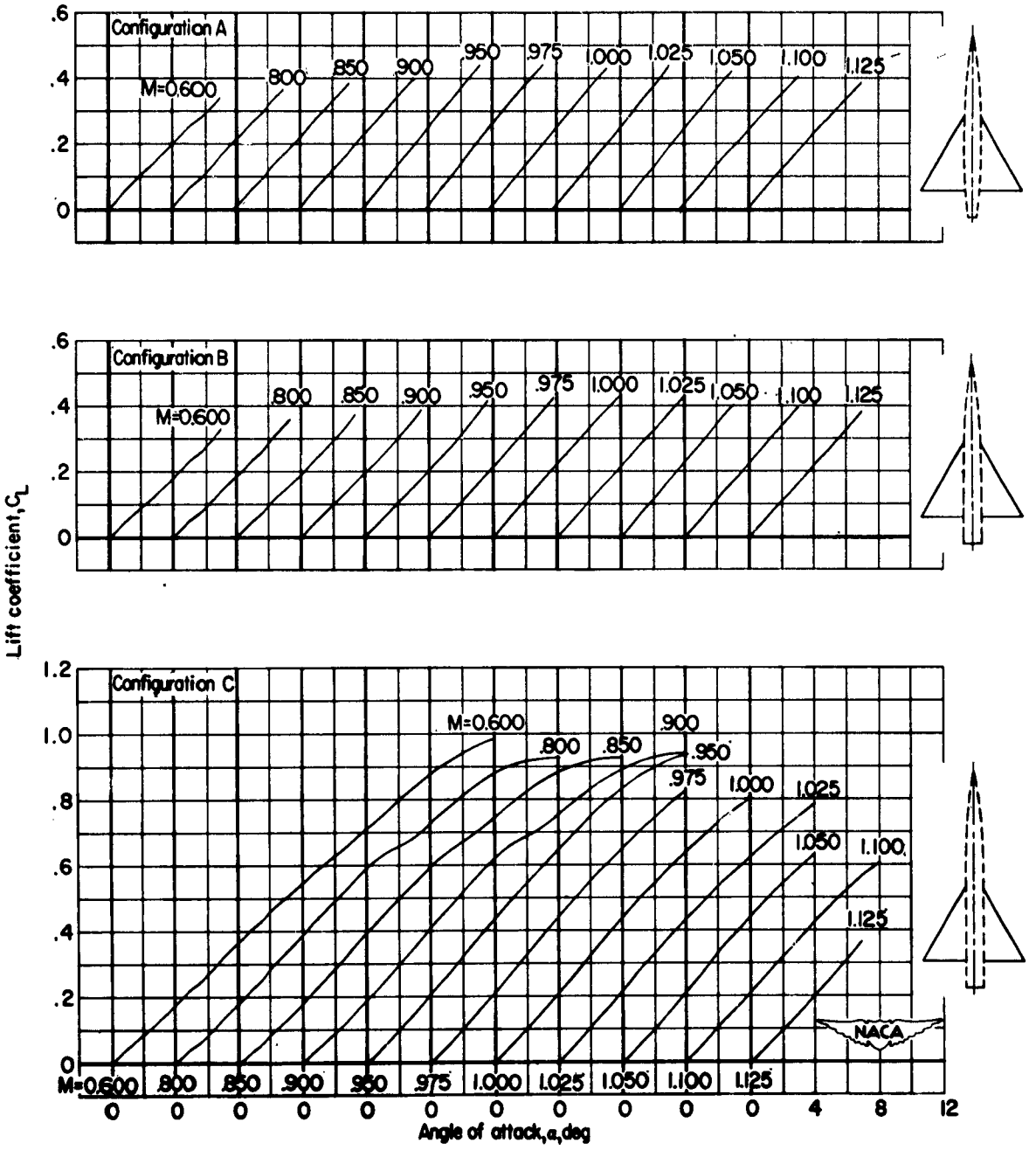

(a) Angle of attack.

Figure 4.- Variation with lift coefficient of force and moment characteristics for wing with wing-fuselage interference.

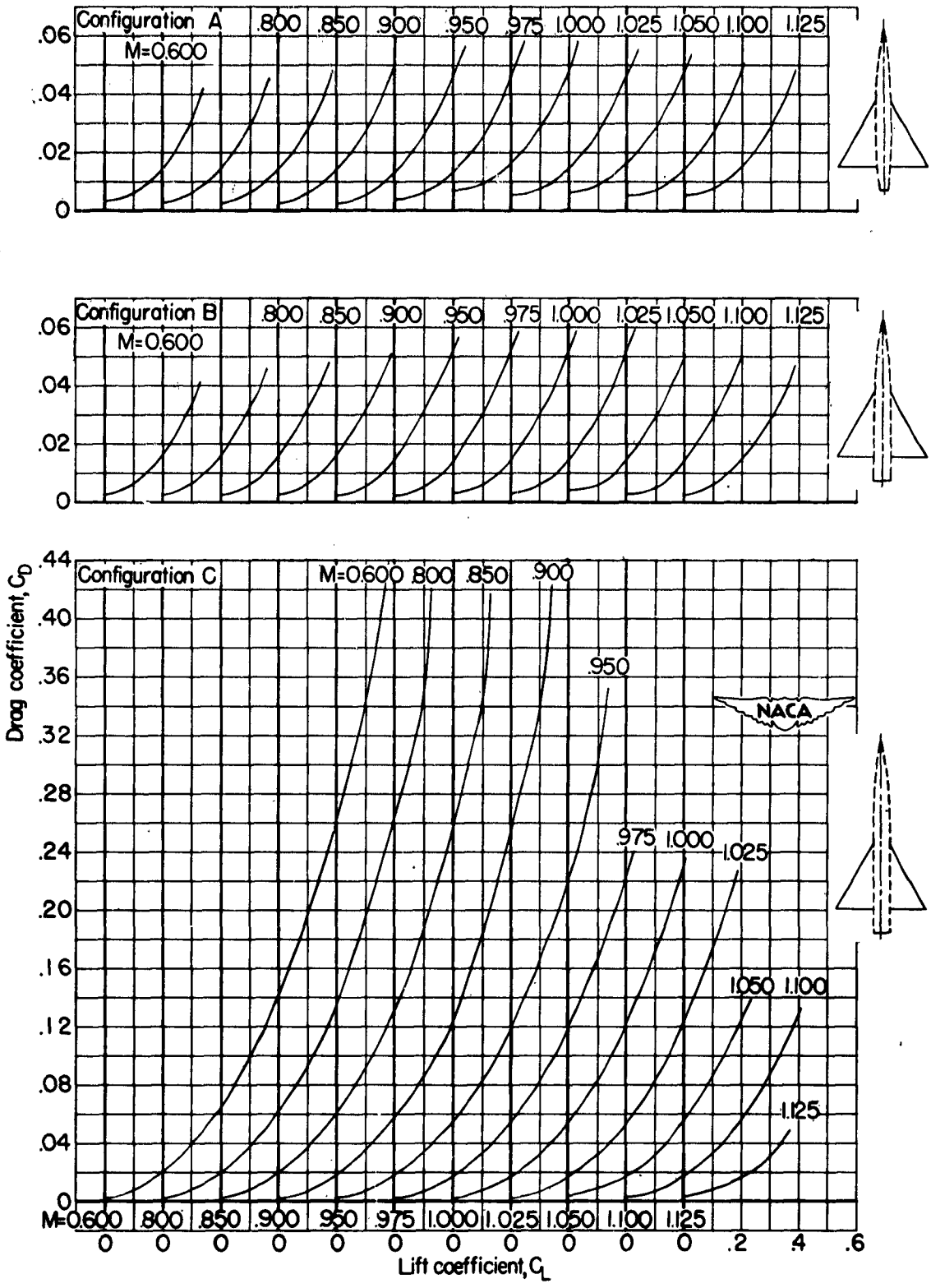

(b) Drag coefficient.

Figure 4.- Continued.

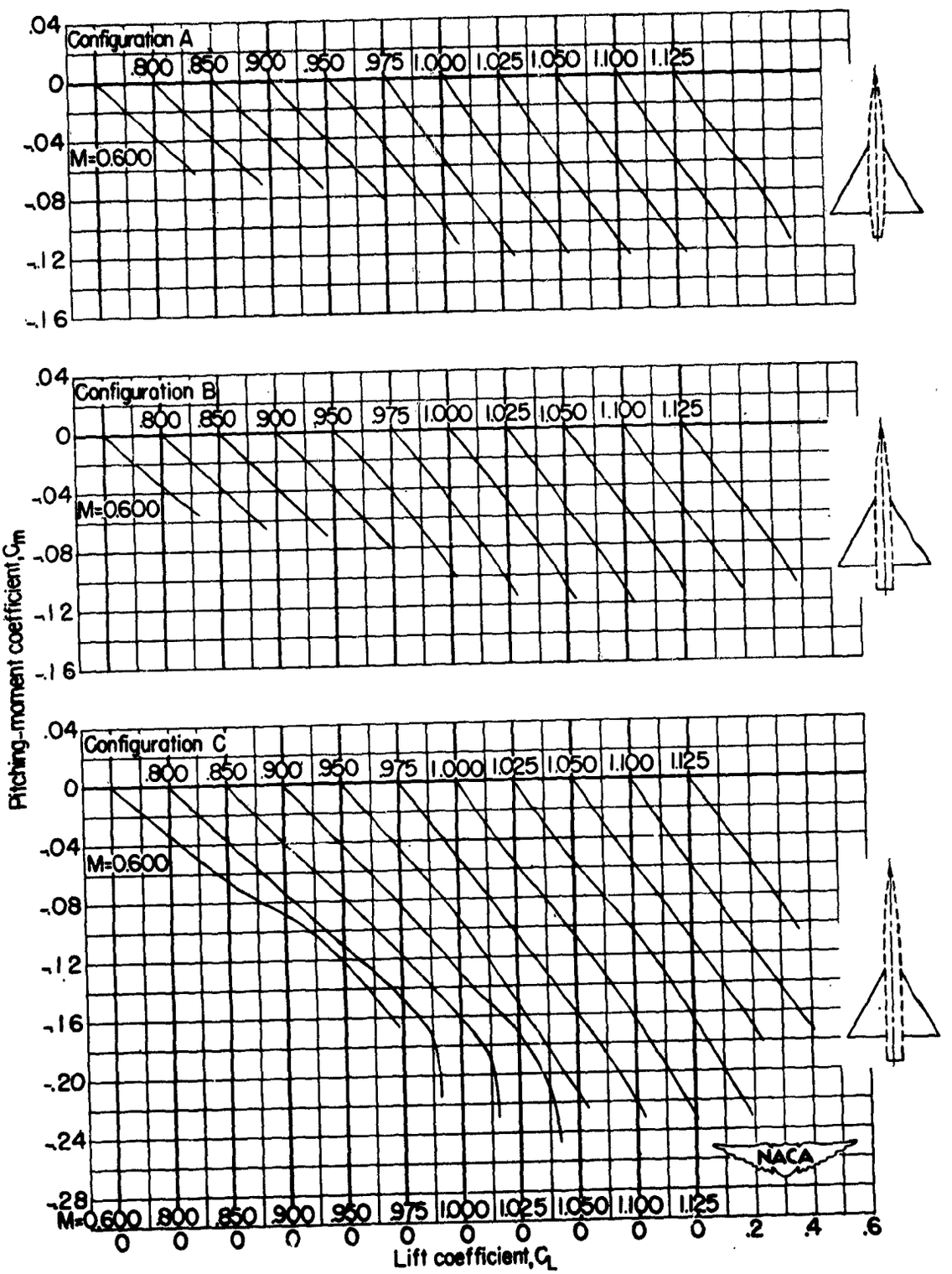

(c) Pitching-moment coefficient.

Figure 4.- Concluded.

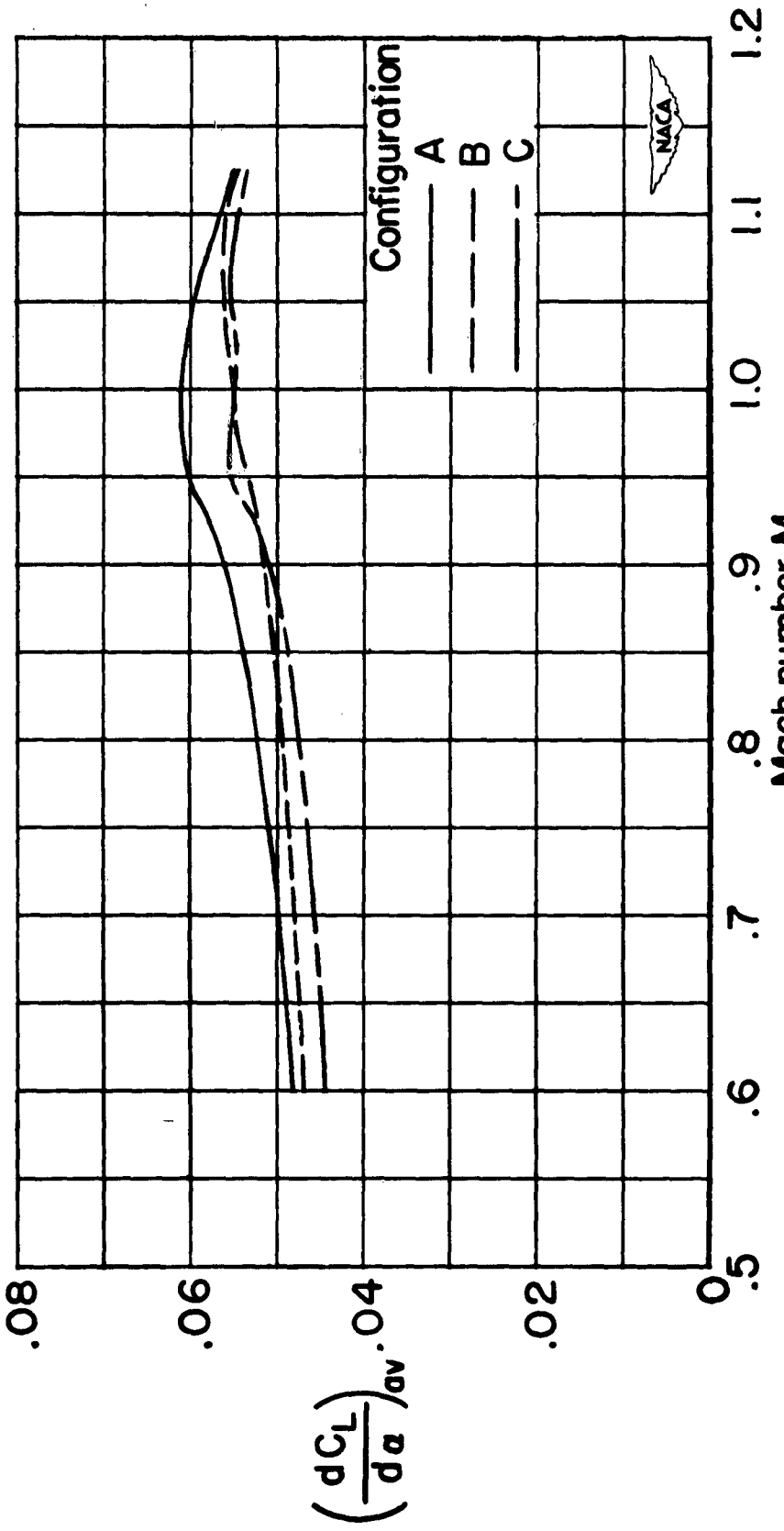

Figure 5.- Variation with Mach number of average lift-curve slope for wing with wing-fuselage interference of the various configurations.

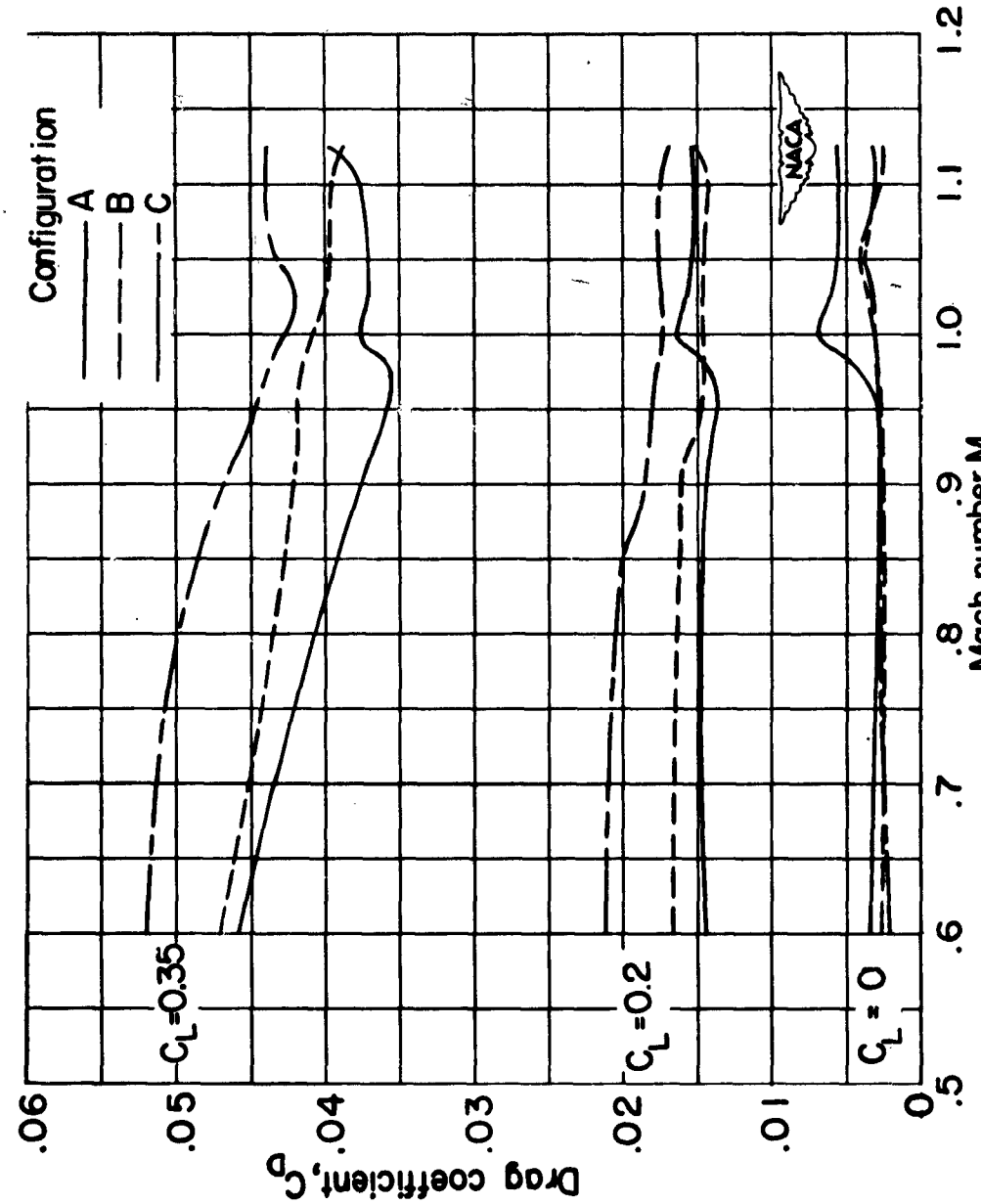

Figure 6.- Variation with Mach number of drag coefficient for wing with wing-fuselage interference of the various configurations at several lift coefficients.

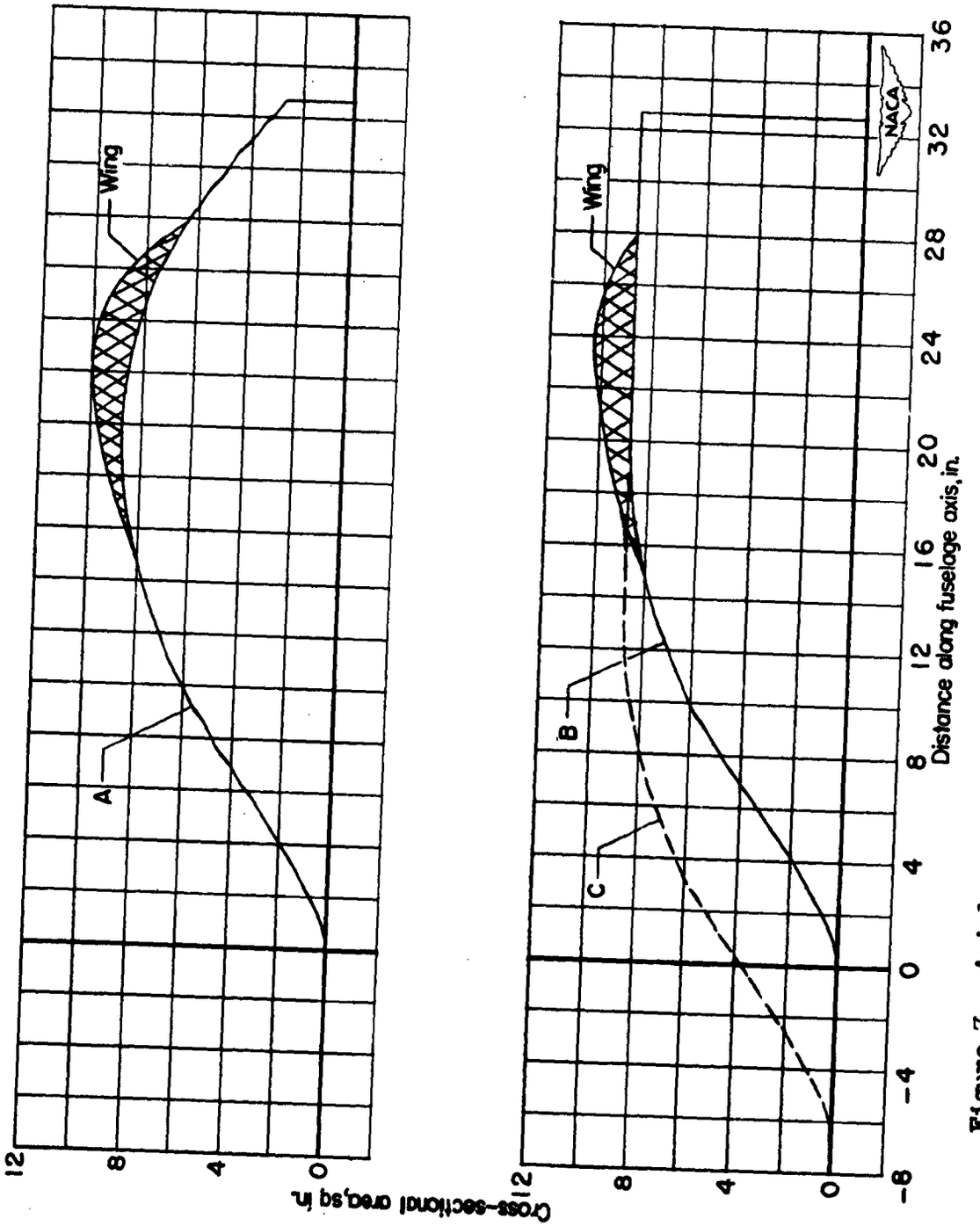

Figure 7.- Axial cross-sectional area developments for the three wing-fuselage configurations.

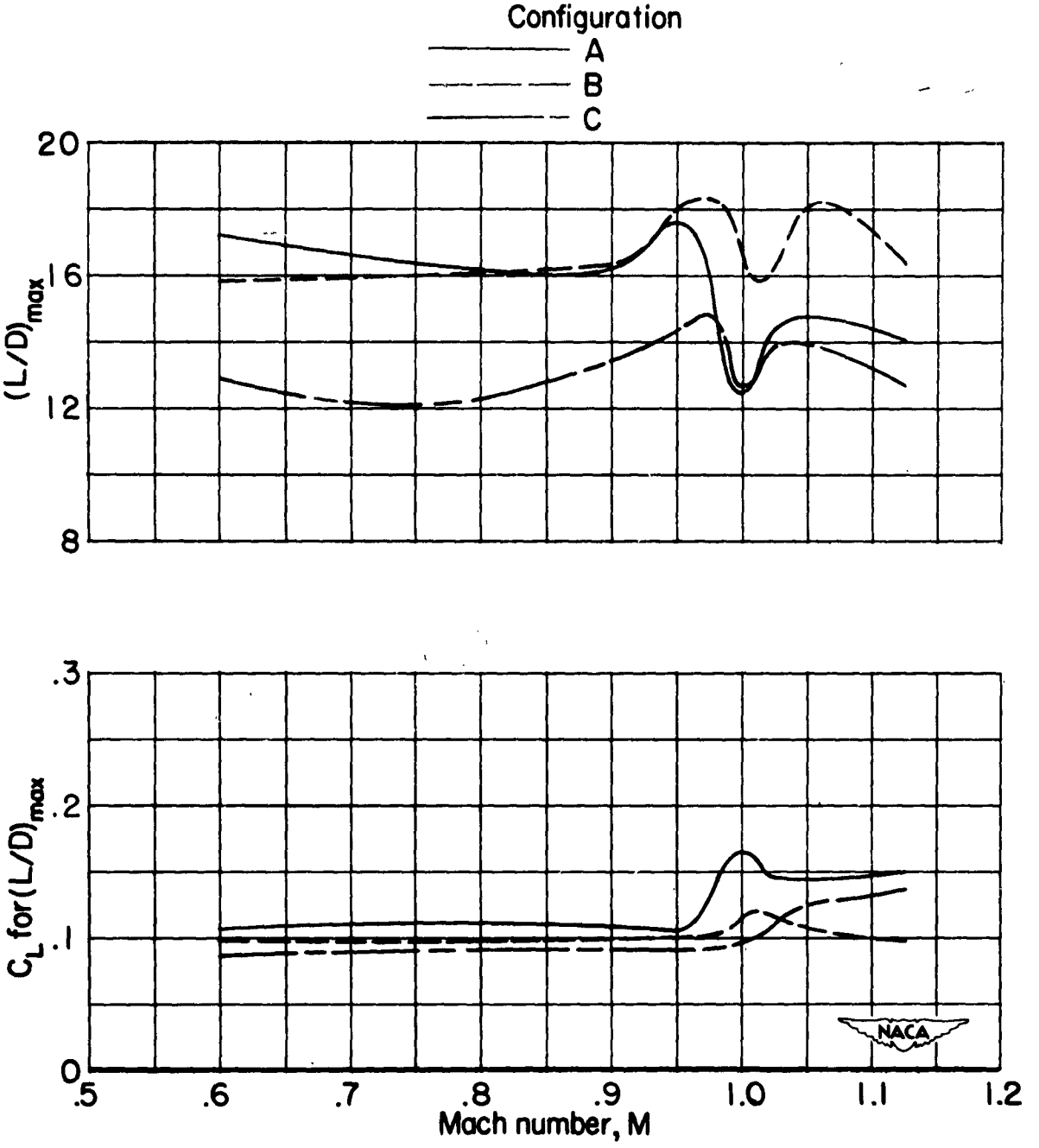

Figure 8.- Variation with Mach number of maximum lift-drag ratio and lift coefficient for maximum lift-drag ratio for wing with interference of the various configurations.

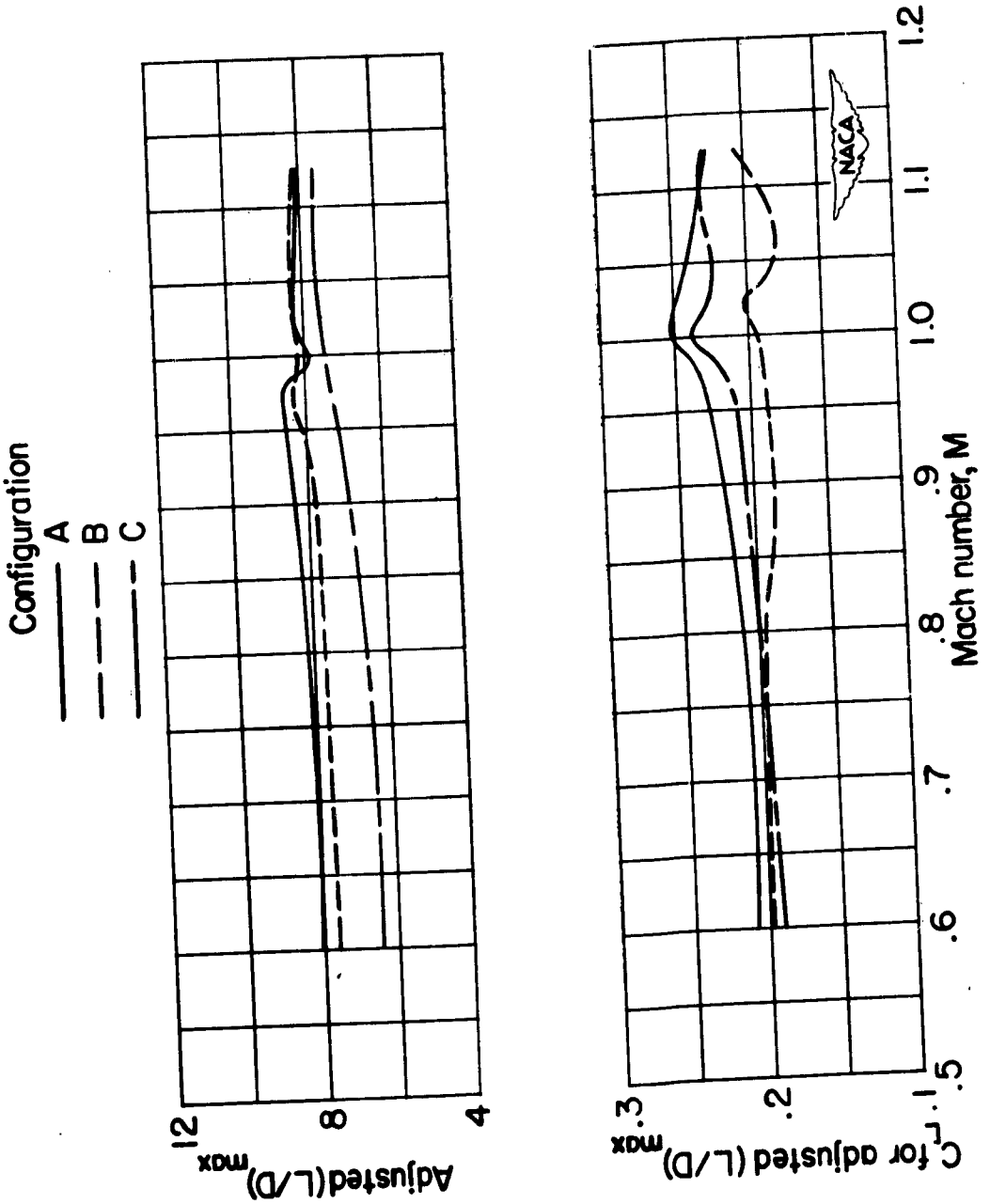

Figure 9.- Variation with Mach number of adjusted maximum lift-drag ratio and lift coefficient for adjusted maximum lift-drag ratio for wing with interference of the various configurations.

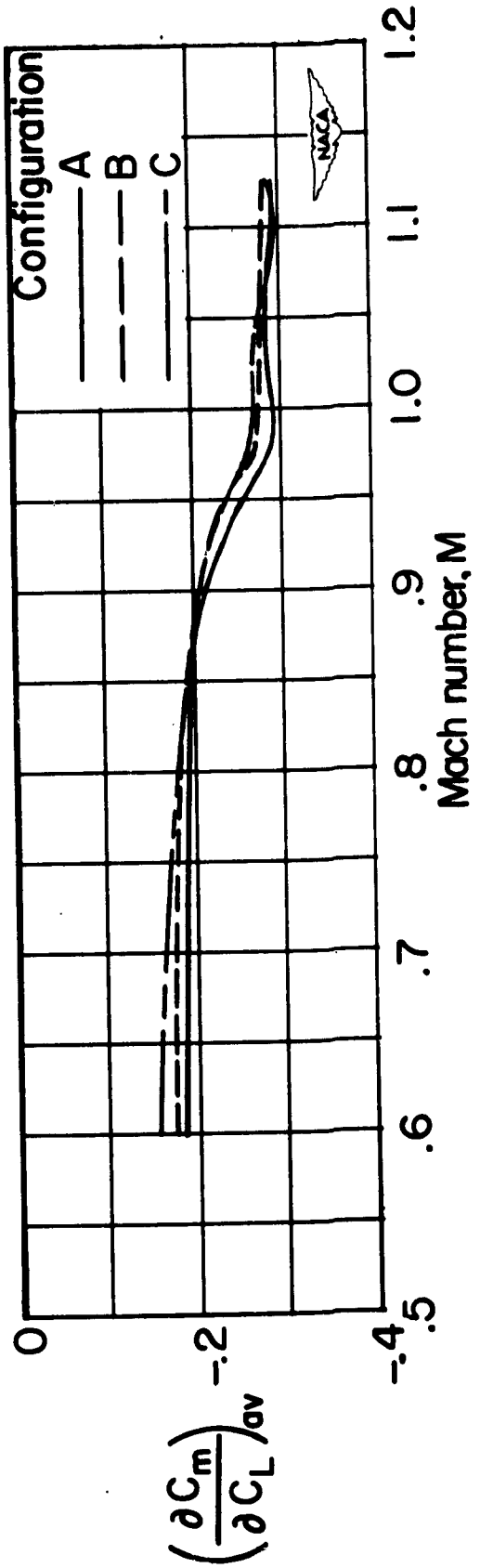

Figure 10.- Variation with Mach number of average static-longitudinal-stability parameter for wing with wing-fuselage interference of the various configurations.

NACA-Langley - 4-6-53 - 325